

# Quasinormal modes of plane-symmetric anti-de Sitter black holes: A complete analysis of the gravitational perturbations

Alex S. Miranda\* and Vilson T. Zanchin†

*Departamento de Física, Universidade Federal de Santa Maria,  
97119-900 Santa Maria, RS, Brazil.*

## Abstract

We study in detail the quasinormal modes of linear gravitational perturbations of plane-symmetric anti-de Sitter black holes. The wave equations are obtained by means of the Newman-Penrose formalism and the Chandrasekhar transformation theory. We show that oscillatory modes decay exponentially with time such that these black holes are stable against gravitational perturbations. Our numerical results show that in the large (small) black hole regime the frequencies of the ordinary quasinormal modes are proportional to the horizon radius  $r_+$  (wave number  $k$ ). The frequency of the purely damped mode is very close to the algebraically special frequency in the small horizon limit, and goes as  $ik^2/3r_+$  in the opposite limit. This result is confirmed by an analytical method based on the power series expansion of the frequency in terms of the horizon radius. The same procedure applied to the Schwarzschild anti-de Sitter spacetime proves that the purely damped frequency goes as  $i(l-1)(l+2)/3r_+$ , where  $l$  is the quantum number characterizing the angular distribution. Finally, we study the limit of high overtones and find that the frequencies become evenly spaced in this regime. The spacing of the frequency per unit horizon radius seems to be a universal quantity, in the sense that it is independent of the wave number, perturbation parity and black hole size.

PACS numbers: 04.70.-s, 04.30.-w, 04.50.+h, 11.25.Hf

---

\* amiranda@mail.ufsm.br

† zanchin@ccne.ufsm.br

## I. INTRODUCTION

The dynamical response of black holes to any external disturbance is dominated, at intermediate times, by a discrete set of damped oscillations called quasinormal modes (QNMs). This result has been verified not only at linearized level, but also in fully numerical simulations for stellar gravitational collapse [1] and collision of two black holes [2]. The possibility of observation in the forthcoming years of the radiation due to the QNMs opens a new perspective for the gravitational wave astronomy. From these observations it will be possible to obtain direct evidence of black holes' existence, as well as to estimate their parameters (mass, electric charge, and angular momentum) [3].

In addition to the astrophysical applications, an interpretation appeared some years ago of the QNMs in terms of the AdS/CFT conjecture [4]. According to this conjecture, there is a correspondence relation (or duality) between string theory in an anti-de Sitter (AdS) spacetime and a conformal field theory (CFT) on the boundary of this space [5, 6]. It implies that a large black hole in the AdS spacetime corresponds to an approximately thermal state in the CFT. Perturbing the black hole is equivalent to perturbing the thermal state, and the perturbation damping time gives the time scale for the return to the thermal equilibrium. Therefore, by computing quasinormal (QN) frequencies in an AdS space it is possible to obtain the thermalization time scale in the strongly coupled CFT.

The early works studying perturbations of AdS black holes considered the evolution of a conformally invariant scalar field in such background spacetimes [7, 8]. After the advent of the AdS/CFT conjecture, QNMs of spacetimes with a negative cosmological constant, such as Kottler (also called Schwarzschild-AdS) [4, 9, 10, 11, 12, 13, 14, 15], Reissner-Nordström-AdS [16, 17, 18, 19, 20] and Kerr-AdS [21, 22, 23], were computed for different fields, dimensions, and boundary conditions. Within this program, other kinds of black hole solutions were also analyzed. For instance, in the Bañados-Teitelboim-Zanelli solution [24], analytical expressions for the QN frequencies presented exact agreement with the poles of the retarded correlation function in the dual CFT [25, 26]. This result provided an important quantitative test of the AdS/CFT correspondence. As a complement to the aforementioned studies, analyses of the time evolution of some fields in asymptotically AdS backgrounds have been performed [27, 28, 29, 30]. More recently, the conjecture relating the highly damped QNMs to black hole area quantization has motivated a search for QN frequencies

with large imaginary parts also in asymptotically AdS spacetimes [31, 32, 33, 34, 35, 36].

The studies of perturbations in AdS spacetimes were also extended to black holes with nonspherical topology. In Ref. [8] the evolution of a conformal scalar field in the family of topological backgrounds was investigated, which includes the plane-symmetric black hole as one of its members, while in Ref. [29] the case of a nonminimally coupled scalar field in the same kind of spacetimes was considered. Lately, the lowest QN frequencies associated with the scalar, electromagnetic, and gravitational perturbations of the plane-symmetric black hole background were computed [37]. The study of the scalar and electromagnetic fields was relatively complete. However, important questions were left without answers in connection with the gravitational perturbations. For instance, what are the wave equations governing general metric perturbations? What is the physical interpretation of the modes with different wave numbers? What are the QN frequencies in the intermediate and small black hole regimes? What is the relation between these frequencies and the wave number? Why is the pure imaginary frequency not proportional to the horizon radius in the large black hole limit as it happens for ordinary modes? Is there some relation between the latter and the algebraically special frequency? And what is the behavior of the QNM spectrum in the regime of highly damped overtones?

The objective of the present work is answering most of the previous questions as well as other ones that appeared during this work. Some of the conclusions drawn here are extended to the Schwarzschild-AdS black hole. The plan of this paper is the following. In Sec. II, we write the equations defining the background spacetime in a Newman-Penrose (NP) null tetrad frame [38]. In Sec. III, we obtain Schrödingerlike equations governing the axial and polar perturbations. In Sec. IV, we define the QNM boundary conditions to be used and prove the black holes stability against perturbations with a non-negative potential. A brief description of the Horowitz-Hubeny method (Sec. V) follows, as well as subsequent exposition of the QN frequency values for different horizon radii and wave numbers (Sec. VI). Then, we study the large black hole limit of the axial QNMs (Sec. VII) and the non-QN character of the algebraically special frequency (Sec. VIII). Finally, we conclude by summarizing and commenting the main results (Sec. IX).

Throughout this work, we use the geometric system of units in which the speed of light and the Newton's gravitational constant are set to unity. The background spacetime, moreover, has a natural lengthscale given by the AdS radius  $R = \sqrt{3/|\Lambda_c|}$ , where  $\Lambda_c$  is the

negative cosmological constant. Here we choose the length unit so that  $R = 1$  and measure everything in terms of the AdS radius. In relation to notation, the asterisk (\*) denotes complex conjugation and the definition of the NP quantities follows Ref. [39].

## II. THE BLACK HOLE SPACETIME

With the aim of investigating the evolution of linear gravitational perturbations in the background of a plane-symmetric AdS black hole [40], we summarize here the basic properties of such a spacetime. The metric may be written in the form

$$ds^2 = f(r)dt^2 - f(r)^{-1}dr^2 - r^2(d\varphi^2 + dz^2), \quad (1)$$

where

$$f(r) = r^2 - 4M/r.$$

There is an event horizon at  $r = r_+ = (4M)^{1/3}$ , and an essential singularity at  $r = 0$ . Depending on the ranges of coordinates  $\varphi$  and  $z$ , the metric may represent a cylindrical ( $0 \leq \varphi < 2\pi$ ,  $-\infty < z < +\infty$ ), toroidal ( $0 \leq \varphi, z < 2\pi$ ) or planar ( $-\infty < \varphi, z < +\infty$ ) black hole spacetime. For the torus,  $M$  is related to the ADM system mass [41]; for the cylinder, to the mass per length unit of  $z$  line [42, 43]; and for the plane, to the mass per area unit of the  $\varphi - z$  plane [44].

According to the Petrov classification, the above metric (1) is algebraically type D. It is then convenient to define the NP quantities in terms of a Kinnersley-like null frame [45]. In this case, the two real vectors of such a frame,  $D$  and  $\Delta$ , are chosen to lie, respectively, on the ingoing and outgoing radial null geodesics and are defined by

$$D = l^\mu \partial_\mu = \frac{1}{f}(\partial_t + f\partial_r), \quad (2)$$

$$\Delta = n^\mu \partial_\mu = \frac{1}{2}(\partial_t - f\partial_r), \quad (3)$$

which are the double principal null directions of the Weyl tensor. In order to complete the frame basis we have the vector

$$\delta = m^\mu \partial_\mu = \frac{1}{r\sqrt{2}}(\partial_\varphi + i\partial_z), \quad (4)$$

and its complex conjugate  $\delta^* = m^{*\mu} \partial_\mu$ . Both of these vectors,  $m^\mu$  and  $m^{*\mu}$ , are orthogonal to  $l^\mu$  and  $n^\mu$ , and satisfy the normalization condition  $m^\mu m_\mu^* = -1$ . With the chosen tetrad

basis, the only nonvanishing spin coefficients are

$$\rho = -1/r, \quad \mu = -f/2r, \quad \gamma = (r^3 + 2M)/2r^2, \quad (5)$$

and the only nonvanishing Weyl and Ricci scalars are

$$\Psi_2 = -2M/r^3, \quad \Lambda = 1/2. \quad (6)$$

### III. THE WAVE EQUATIONS

Here the equations for the linear gravitational perturbations are obtained by using the NP formalism, which allows us to investigate general properties of such perturbations without any further simplifying assumption. In this approach, changes in the metric coefficients are directly related to changes in the tetrad null vectors. Furthermore, perturbations in the vectors  $l^\mu$ ,  $n^\mu$  and  $m^\mu$  lead to first order alterations in Weyl and Ricci scalars, and also in the spin coefficients. The full system of linearized perturbation equations is obtained by expanding the complete NP equations on the plane-symmetric black hole background, and retaining only the first order terms in the perturbation functions.

Generally, the linearized NP equations form a large system of coupled equations whose solutions are difficult to be found. However, for Petrov type D vacuum spacetimes, the problem reduces to solving a pair of decoupled equations for the gauge and tetrad invariants  $\Psi_0$  and  $\Psi_4$  [46]. In the present case, these equations assume the simple forms

$$[(D - 4\rho - \rho^*)(\Delta - 4\gamma + \mu) - \delta\delta^* - 3\Psi_2]\Psi_0 = 0, \quad (7)$$

$$[(\Delta + 3\gamma - \gamma^* + 4\mu + \mu^*)(D - \rho) - \delta^*\delta - 3\Psi_2]\Psi_4 = 0. \quad (8)$$

The foregoing equations are already linearized since the Weyl scalars  $\Psi_0$  and  $\Psi_4$  vanish in the equilibrium state, and then they are to be considered first order perturbations. The other quantities take their unperturbed values given in Eqs. (2)-(6).

The background symmetries, together with the perturbation equations (7) and (8), indicate that each one of the perturbation functions  $\Psi_0$  and  $\Psi_4$  can be written as a product of four different functions depending upon only one of the coordinates  $t$ ,  $r$ ,  $\varphi$ , and  $z$ . Moreover, due to the wavelike character of the equations, the dependence of these functions on the coordinates  $t$ ,  $\varphi$  and  $z$  is of the form  $\exp[i(\omega t + k_\varphi\varphi + k_z z)]$ , where  $\omega$  is the frequency, and  $k_\varphi$  and  $k_z$  are wave numbers which may assume discrete or continuous values, depending on

whether  $\varphi$  and  $z$  are compact or noncompact coordinates, respectively. The radial functions, in turn, are conveniently written as

$$\Psi_0(r) = r^{-1}f^{-2}Y_{+2}(r), \quad \Psi_4(r) = r^{-1}Y_{-2}(r),$$

where the subscripts  $\pm 2$  are related to the spin weight and to the conformal weight of the Weyl scalars  $\Psi_0$  and  $\Psi_4$ .

The resulting equations for  $Y_{\pm 2}$  take the following standard form:

$$\Lambda^2 Y_{\pm 2} + P\Lambda_{\mp} Y_{\pm 2} - QY_{\pm 2} = 0, \quad (9)$$

where we introduced the differential operators

$$\Lambda_{\pm} = \frac{d}{dr_*} \pm i\omega, \quad \Lambda^2 = \frac{d^2}{dr_*^2} + \omega^2.$$

Here  $r_*$  is the tortoise coordinate, defined in such a way that  $dr/dr_* = f(r)$ , and

$$P = \frac{d}{dr_*} \ln \left( \frac{r^4}{f^2} \right), \quad Q = \frac{f}{r^3}(k^2 r + 12M),$$

with  $k^2 = k_{\varphi}^2 + k_z^2$ .

The Chandrasekhar transformation theory [39] can now be used to transform Eqs. (9) into one-dimensional Schrödingerlike equations of the form

$$\Lambda^2 Z^{(\pm)} = V^{(\pm)} Z^{(\pm)}. \quad (10)$$

This is done by means of the substitutions

$$\begin{aligned} Y_{+2} &= V^{(\pm)} Z^{(\pm)} + (W^{(\pm)} + 2i\omega)\Lambda_+ Z^{(\pm)}, \\ Y_{-2} &= V^{(\pm)} Z^{(\pm)} + (W^{(\pm)} - 2i\omega)\Lambda_- Z^{(\pm)}, \end{aligned}$$

whose inverse transformation gets the form

$$\begin{aligned} K^{(\pm)} Z^{(\pm)} &= \frac{r^4}{f^2} Q Y_{+2} - \frac{r^4}{f^2} (W^{(\pm)} + 2i\omega)\Lambda_- Y_{+2}, \\ K^{(\mp)} Z^{(\pm)} &= \frac{r^4}{f^2} Q Y_{-2} - \frac{r^4}{f^2} (W^{(\pm)} - 2i\omega)\Lambda_+ Y_{-2}, \end{aligned}$$

where

$$K^{(\pm)} = k^4 \pm 24i\omega M. \quad (11)$$

In the foregoing equations, the potential functions  $V^{(\pm)}$  are given by

$$V^{(+)} = \frac{f}{r^3} \left[ \frac{576M^3 + 12k^4Mr^2 + k^6r^3 + 144M^2r(k^2 + 2r^2)}{(k^2r + 12M)^2} \right], \quad (12)$$

$$V^{(-)} = \frac{f}{r^3}(k^2r - 12M), \quad (13)$$

while the auxiliary functions  $W^{(\pm)}$  are, respectively,

$$W^{(+)} = -\frac{12M(2r^3 + k^2r + 4M)}{r^2(k^2r + 12M)}, \quad W^{(-)} = -\frac{12M}{r^2}.$$

The meaning of the signs  $(\pm)$  comes from the metric approach to the perturbation problem, as it was performed in Ref. [37]. They are related to the parity property of the perturbed metric functions under the exchange  $\varphi \rightarrow -\varphi$  (or  $z \rightarrow -z$ ). The variable  $Z^{(+)}$  represents the polar (even) perturbations, while  $Z^{(-)}$  represents the axial (odd) ones.

In a certain sense, the wave equations (10) can be thought of as a generalization to those found by Cardoso and Lemos [37]. Here the perturbations depend on both coordinates  $\varphi$  and  $z$ , while in the aforementioned work the analysis was restricted to  $z$ -independent metric variations. This is equivalent to the vanishing of the wave number  $k_z$ , resulting in  $k^2 = k_\varphi^2$ . However, the plane symmetry of the background spacetime renders possible to find new coordinates  $(\varphi', z')$  in such a way that one of the wave numbers,  $k'_\varphi$  or  $k'_{z'}$ , is zero. That is to say, it is always possible to find a coordinate system in which the perturbations depend only on two space coordinates ( $r$  and  $\varphi$ , or  $r$  and  $z$ ).

Another result derived from the above analysis is related to the Starobinsky constant [47],  $|\mathcal{C}|^2 = K^{(+)}K^{(-)}$ , where  $K^{(\pm)}$  are given by Eq. (11). The solutions of  $|\mathcal{C}|^2 = 0$  correspond to algebraically special frequencies in the sense of Chandrasekhar [48]. As we shall see in Sec. VI, one of such solutions, given by

$$\omega_a = i \frac{k^4}{24M} = i \frac{k^4}{6r_+^3}, \quad (14)$$

appears in the numerical results in connection to the purely damped QNMs. The properties of the axial perturbations related to these algebraically special modes are analyzed in some detail in Sec. VIII.

#### IV. QNM ANALYTICAL PROPERTIES

To solve the wave equations (10) we must impose boundary conditions on the possible solutions. First, however, consider the case of the asymptotically flat Schwarzschild spacetime. Gravitational perturbations lead to Schrödingerlike equations whose potentials vanish at infinity and at the event horizon. Hence, close to these extremities, the solutions are plane waves,  $Z \rightarrow e^{\pm i\omega r_*}$ , where the  $r_*$  coordinate ranges from  $-\infty$  to  $+\infty$ . QNMs are then defined as solutions which are purely ingoing waves at the horizon,  $Z \rightarrow e^{+i\omega r_*}$ , and purely outgoing waves at infinity,  $Z \rightarrow e^{-i\omega r_*}$ . These requirements are satisfied only for a discrete set of complex  $\omega$  called the quasinormal frequencies.

In asymptotically AdS spacetimes, we keep the requirement of purely ingoing waves at the horizon. In the meantime, since now the tortoise coordinate  $r_*$  takes a finite value at spatial infinity, the boundary condition at infinity must be changed. This can be Dirichlet, Neumann, or Robin boundary condition, depending on whether the field, its derivative, or a combination of both vanishes, respectively. Here, as in most of the literature, we adopt Dirichlet boundary conditions, since these lead to energy conservation in the field theory on AdS space [49] (for alternative boundary conditions see Ref. [12]).

Having defined the QNMs, we show below that the imaginary part of the QN frequencies is positive for non-negative potentials. The demonstration follows the one carried out in the Schwarzschild-AdS case by Cardoso and Lemos [9]. Initially, we exchange the variable  $Z$  by  $\phi = e^{-i\omega r_*} Z$ , so that Eq. (10) becomes

$$f \frac{d^2 \phi}{dr^2} + \left( \frac{df}{dr} + 2i\omega \right) \frac{d\phi}{dr} - \frac{V}{f} \phi = 0, \quad (15)$$

where  $Z$ ,  $\phi$  and  $V$  stand for both perturbation types, the polar ( $Z^{(+)}$ ,  $\phi^{(+)}$ ,  $V^{(+)}$ ) and the axial ones ( $Z^{(-)}$ ,  $\phi^{(-)}$ ,  $V^{(-)}$ ).

Near the horizon and at infinity, the solutions  $\phi$  satisfying the QNM boundary conditions are given, respectively, by

$$\phi_{r_+} = A \frac{(C_1/3r_+)^{i\omega/3r_+}}{\Gamma[1 + (2i\omega/3r_+)]}, \quad (16)$$

$$\phi_\infty = B e^{i\omega/r} \sin \left( \sqrt{\omega^2 - C_2/r} \right), \quad (17)$$

where  $A$  and  $B$  are arbitrary constants, and  $C_1 = V(r_+)/f(r_+)$  and  $C_2 = V(\infty)$  are definite constants whose values depend on the perturbation type.



Now we multiply Eq. (15) by  $\phi^*$  and integrate by parts using the asymptotic solutions (16) and (17). After some algebra we obtain

$$\int_{r_+}^{\infty} \left[ f \left| \frac{d\phi}{dr} \right|^2 + \frac{V}{f} |\phi|^2 \right] dr = \frac{|\omega|^2 |\phi(r_+)|^2}{\text{Im}(\omega)}. \quad (18)$$

Since  $f(r)$  assumes only positive values outside of the black hole, the sign of the quantity on the left hand side of Eq. (18) depends crucially on the sign of the potential  $V(r)$ . For non-negative  $V$ , it follows that the imaginary part of the QN frequencies is positive,  $\Im(\omega) > 0$ . Moreover, it is seen from Eq. (12) that  $V^{(+)}$  is positive in the region  $r_+ < r < \infty$  for any  $k$  and  $r_+$ , and then we conclude that the plane-symmetric AdS black holes are stable against polar perturbations. The same is true for axial perturbations as far as the wave numbers are restricted by  $k \geq \sqrt{3}r_+$ . On the other hand, for  $k < \sqrt{3}r_+$ , the potential  $V^{(-)}$  takes negative values and the theorem cannot be applied.

Another interesting property of frequencies associated to perturbations of a plane-symmetric black hole comes from the particular symmetry of such a background. This symmetry allows us to rescale  $\omega$ ,  $k$  and  $r_+$  by a pure scale transformation of coordinates  $t = at'$ ,  $\varphi = a\varphi'$ ,  $z = az'$ , and  $r = r'/a$ , where  $a$  is a constant [4]. It implies that the frequency is a first degree homogeneous function of its parameters:  $\omega(ar_+, ak) = a\omega(r_+, k)$ . In particular, we can take  $a = k_0/k$  so that

$$\omega(r_+, k) = \frac{k}{k_0} \omega\left(\frac{k_0}{k} r_+, k_0\right). \quad (19)$$

Then, after computing the QN frequencies for a given  $k$ , e. g., for  $k = k_0$ , and for different values of  $r_+$ , we can obtain  $\omega(r_+, k)$  by using the previous equation, and the values of  $\omega$  for a fixed wave number  $k$  are naturally divided into three different regimes: large ( $r_+ \gg k$ ), intermediate ( $r_+ \sim k$ ) and small ( $r_+ \ll k$ ) black holes. In the large (small) black hole limit,  $k$  ( $r_+$ ) is negligibly small and it is expected that  $\omega \propto r_+$  ( $\omega \propto k$ ).

We are now in a position to solve the perturbation equations (10) and to find the values of the QN frequencies. This task, however, is more easily done through numerical procedures. Therefore, it is appropriate summarizing here the method used for such a purpose.

## V. THE HOROWITZ-HUBENY METHOD

In the last decades a series of methods has been developed to numerically calculate the QNMs of black holes. Here we briefly describe one of these methods, used in Ref. [4],

which is of particular interest for the present work since it is suited for asymptotically AdS spacetimes. In order to apply such a method we rewrite here the perturbation equations in the appropriate form.

By introducing the independent variable  $x = 1/r$ , Eq. (15) becomes

$$(x^3 - x_+^3) \frac{d^2 \phi}{dx^2} + (3x^2 + 2i\omega x_+^3) \frac{d\phi}{dx} + \tilde{V} \phi = 0, \quad (20)$$

where  $x_+ = 1/r_+$  and  $\tilde{V}(x) = x_+^3 V/fx^2$ , with  $V$  and  $f$  now being considered as functions of  $x$ . The foregoing equation has a regular singular point ( $x = x_+$ ) in the region of interest,  $0 \leq x \leq x_+$ . Then, by Fuchs theorem, any solution of (20) can be written as a Fröbenius series [50]. The behavior of the solutions near the horizon may be explored by writing  $\phi(x) = (x - x_+)^{\alpha}$ , where  $\alpha$  is a constant to be determined. By substituting this expression into Eq. (20) and keeping terms only to the leading order, it follows that  $x_+^2 \alpha(3\alpha + 2i\omega x_+) = 0$ , which has the roots  $\alpha = 0$  and  $\alpha = -2i\omega/3r_+$ . These roots correspond exactly to the ingoing and outgoing waves at the horizon, respectively [4]. Since we want only ingoing modes, we take  $\alpha = 0$  and look for solutions of the form

$$\phi(x) = \sum_{m=0}^{\infty} a_m (x - x_+)^m. \quad (21)$$

Substituting Eq. (21) into (20), we find expressions for the  $a_m$ 's in terms of the frequency  $\omega$  (and of the parameters  $k$  and  $x_+$ ). Then, imposing the boundary condition at infinity,  $\phi(0) = 0$ , we obtain

$$\sum_{m=0}^{\infty} a_m(\omega) (-x_+)^m = 0. \quad (22)$$

Thus, the problem of finding QN frequencies has been reduced to that of obtaining the roots of the infinite-order polynomial equation (22). Of course, we cannot carry out numerically the full sum in expression (22). In effect we truncate the series after a large number of terms and look for the zeros of this partial sum. The precision of the results is then verified by computing the relative variation between the zeros as we perform higher partial sums. We stop our search once we have a 6 decimal digit precision. For each pair of  $k$  and  $r_+$ , we find a set of QN frequencies (out of the infinity of possible frequencies). These frequencies are labeled as usual with the principal quantum number  $n$  and ordered in a set beginning with the roots with the lowest imaginary parts.

## VI. NUMERICAL RESULTS AND ANALYSIS

We use the Horowitz-Hubeny procedure described above to compute the gravitational QNMs of plane-symmetric AdS black holes. As it happens to other AdS black holes, there are *purely damped modes*, whose frequencies are pure imaginary numbers, in addition to the *ordinary modes*, the frequencies of which also have nonzero real parts which are responsible for the oscillatory behavior of the perturbations.

As mentioned earlier, the numerical analysis is divided into three different regimes according to the ratio  $r_+/k$  values. That is to say, we have (i) large black holes when the ratio  $r_+/k$  is large compared to unity; (ii) intermediate black holes if  $r_+/k$  is of the order of unity; and (iii) small black holes when  $r_+/k$  is small compared to unity.

It is also worth mentioning here that some numerical analysis of the gravitational QNMs was done in Ref. [37]. However, such a study was restricted mainly to the large black hole regime for a specific value of  $k$ , without generalizations for a generic wave number. In what follows, we perform a more detailed analysis, including small and intermediate black holes, and extend implicitly the numerical results to all values of  $k$ . We also search the QN frequency values in the limit of highly damped overtones.

### A. Ordinary quasinormal modes

To begin with, we discuss the case of regular (ordinary) QNMs for which the frequencies have nonvanishing real and imaginary parts,  $\omega = \omega_r + i\omega_i$ . We list some numerical results of the lowest quasinormal frequencies for  $k = 2$  and some selected values of  $r_+$ . The computed quantities include both the axial and polar perturbations, and the three regimes defined above. The data for large, intermediate, and small black holes are shown, respectively, in Tables I, II, and III.

The first feature to be noticed is that, contrary to the asymptotically flat space case, the axial and polar perturbations no longer have the same spectra. In fact, the isospectrality is only restored in the large and small black hole limits (see also Refs. [9, 18]).

The displayed numerical results also allow us to obtain the  $k$  dependence of the modes on basis of the homogeneity property of the function  $\omega(r_+, k)$ , as represented by Eq. (19).

| $r_+$ | Axial      |            | Polar      |            |
|-------|------------|------------|------------|------------|
|       | $\omega_r$ | $\omega_i$ | $\omega_r$ | $\omega_i$ |
| 1000  | 1849.42    | 2663.84    | 1849.45    | 2663.85    |
| 500   | 924.710    | 1331.92    | 924.727    | 1331.92    |
| 100   | 184.948    | 266.384    | 184.963    | 266.351    |
| 50    | 92.4820    | 133.189    | 92.5134    | 133.124    |
| 10    | 18.5492    | 26.6228    | 18.6960    | 26.2961    |
| 5     | 9.35491    | 13.2880    | 9.62439    | 12.6329    |

TABLE I: The lowest ordinary QN frequencies for  $k = 2$  and several values of  $r_+$  in the large black hole regime.

| $r_+$ | Axial      |            | Polar      |            |
|-------|------------|------------|------------|------------|
|       | $\omega_r$ | $\omega_i$ | $\omega_r$ | $\omega_i$ |
| 2     | 3.92888    | 5.24698    | 4.06031    | 3.84425    |
| 1.6   | 3.21225    | 4.15458    | 3.21731    | 2.78751    |
| 1.2   | 2.44666    | 2.99891    | 2.52608    | 1.92268    |
| 1     | 2.04735    | 2.21550    | 2.30526    | 1.55218    |
| 0.8   | 2.05189    | 1.41550    | 2.18361    | 1.19971    |
| 0.4   | 2.09860    | 0.520025   | 2.10247    | 0.511896   |

TABLE II: The lowest ordinary QN frequencies for  $k = 2$  and several values of  $r_+$  in the intermediate size black hole regime.

More specifically, the  $k \neq 0$  associated frequency can be found by means of the relation

$$\omega(r_+, k) = \frac{k}{2} \omega\left(2 \frac{r_+}{k}, 2\right). \quad (23)$$

For large black holes, our results are in perfect agreement with those found in Ref. [37]. Axial and polar perturbations have real and imaginary parts of the fundamental frequencies given approximately by  $\omega_r = 1.85r_+$  and  $\omega_i = 2.66r_+$ . According to Eq. (23), these linear fits are wave-number independent. They are also equal to those from the large Schwarzschild-AdS black hole [9], as should be expected, since a spherical system approaches a plane one as the radius goes to infinity.

| $r_+$ | Axial      |            | Polar      |            |
|-------|------------|------------|------------|------------|
|       | $\omega_r$ | $\omega_i$ | $\omega_r$ | $\omega_i$ |
| 1/10  | 2.02727    | 0.0916071  | 2.02727    | 0.0915965  |
| 1/12  | 2.02223    | 0.0733694  | 2.02223    | 0.0733649  |
| 1/14  | 2.01866    | 0.0608423  | 2.01866    | 0.0608402  |
| 1/16  | 2.01601    | 0.0517477  | 2.01601    | 0.0517466  |
| 1/18  | 2.01397    | 0.0448789  | 2.01397    | 0.0448783  |
| 1/20  | 2.01236    | 0.0395123  | 2.01236    | 0.0395118  |

TABLE III: The lowest ordinary QN frequencies for  $k = 2$  and several values of  $r_+$  in the small black hole regime.

For small and intermediate black holes, the quasinormal frequencies do not scale with the horizon radius. This is clearly shown in Fig. 1, where we plot the lowest axial and polar frequencies as functions of  $r_+$ , for  $k = 2$  and  $0.1 \leq r_+ \leq 4$ . The exact way the curve  $\omega(r_+)$  deviates from the linear behavior depends on the perturbation parity. Within a certain accuracy, the fundamental frequency starts deviating from the line  $\omega = (1.85 + i2.66)r_+$  around  $r_+ = k/2$  for axial modes, and around  $r_+ = 5k/2$  for polar modes. As the ratio  $r_+/k$  goes to zero, we have  $\omega_r \rightarrow k$  and  $\omega_i \rightarrow 0$ , independently of the perturbation type. In fact, the dependence of  $\omega$  upon  $k$  in the limit of small black holes may be obtained using Eq. (19) which gives  $\omega(r_+, k) \approx \omega(0, k_0) k/k_0 = \text{const.} \times k$ . The numerical analysis shows that for the fundamental mode the proportionality constant is equal to unity. The relation of this result to the pure AdS modes is investigated in Appendix A.

## B. Purely damped modes

Axial perturbations of AdS black holes are known to have special quasinormal modes which are purely damped. In the present case, the values of the associated frequencies,  $\omega = i\omega_s$ , are listed in Table IV for  $k = 2$  and some selected values of  $r_+$ . Once again, the homogeneity property of  $\omega(r_+, k)$  allows us to obtain the  $k$  dependence of the frequency on the basis of relation (23).

For large black holes, our numerical results agree with those presented in Ref. [37]. To

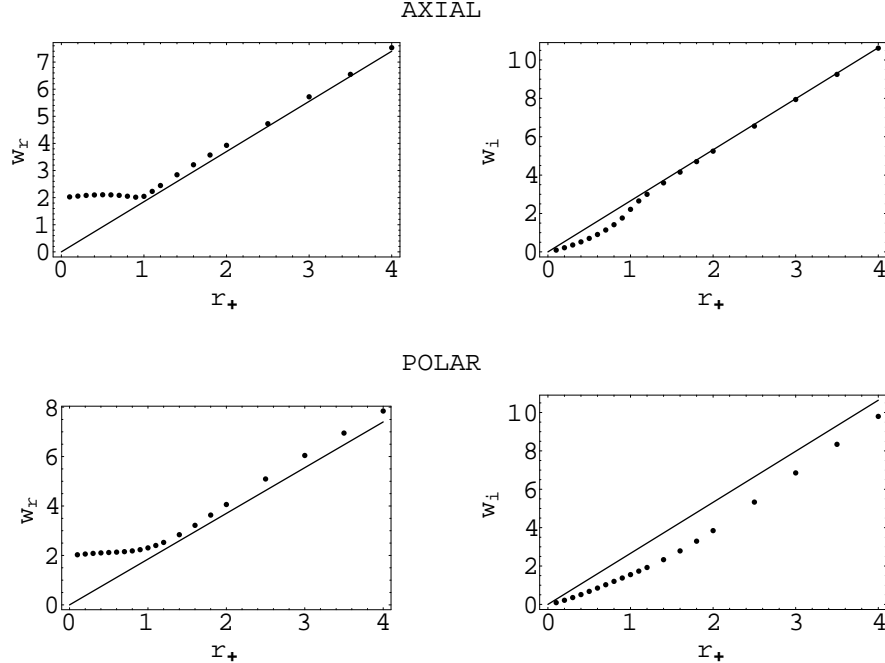


FIG. 1: The frequency of ordinary QNMs for axial and polar perturbations,  $\omega = \omega_r + i\omega_i$ , as a function of the horizon radius  $r_+$  for small and intermediate black holes. The dots represent numerical results, and the solid lines are linear fits. On the left are the real parts ( $\omega_r$ ) with the linear fit  $1.85r_+$ , on the right, the imaginary parts ( $\omega_i$ ), with the fit line  $2.66r_+$ .

a remarkable accuracy, the  $k = 2$  pure imaginary mode is well described by the formula  $\omega_s = 4/3r_+$ . The extension of this fit to any  $k$  leads to  $\omega_s = k^2/3r_+$ . A similar result was already obtained for the Schwarzschild-AdS spacetime by Cardoso *et al* [31]. They found  $\omega_s = (l - 1)(l + 2)/3r_+$ , where  $l$  is the angular momentum of the perturbation. The above two formulas for  $\omega_s$  are just fits to the numerical data, but we were able to find an exact analytical proof for both of them by expanding  $\omega_s$  in a power series of  $1/r_+$ . This study is the subject of the next section.

For intermediate size black holes, the frequency  $\omega_s$  increases faster than  $k^2/3r_+$  as the horizon radius decreases (see Fig. 2). Another special feature of this regime is related to the behavior of the axial potential  $V^{(-)}$  as a function of the coordinate  $r$ . As we go from larger to smaller horizon radii in the plane  $r_+ \times k$ , the straight line  $k = \sqrt{3}r_+$  is the boundary on which the axial potential (13) becomes a non-negative function in the region  $r_+ \leq r < \infty$ . In other words,  $V^{(-)}(r) \geq 0$  at all points outside of a black hole perturbed by an axial

| $r_+$ | $\omega_s$ | $4/3r_+$  | $r_+$ | $\omega_s$ | $r_+$ | $\omega_s$ | $8/3r_+^3$ |
|-------|------------|-----------|-------|------------|-------|------------|------------|
| 100   | 0.0133342  | 0.0133333 | 2.0   | 0.733037   | 0.9   | 3.66330    | 3.65798    |
| 75    | 0.0177794  | 0.0177778 | 1.8   | 0.835965   | 0.7   | 7.77447    | 7.77454    |
| 50    | 0.0266704  | 0.0266667 | 1.6   | 0.978431   | 0.5   | 21.3333    | 21.3333    |
| 25    | 0.0533639  | 0.0533333 | 1.4   | 1.19459    | 0.3   | 98.7654    | 98.7654    |
| 10    | 0.133786   | 0.133333  | 1.2   | 1.58723    | 0.2   | 333.333    | 333.333    |
| 5     | 0.270361   | 0.266667  | 1.0   | 2.64636    | 0.1   | 2666.67    | 2666.67    |

TABLE IV: The pure imaginary QN frequency for  $k = 2$  and some selected values of  $r_+$ . The formula  $4/3r_+$  is a fit valid for large black holes, while  $8/3r_+^3$  is the magnitude of the algebraically special frequency  $\omega_a$ .

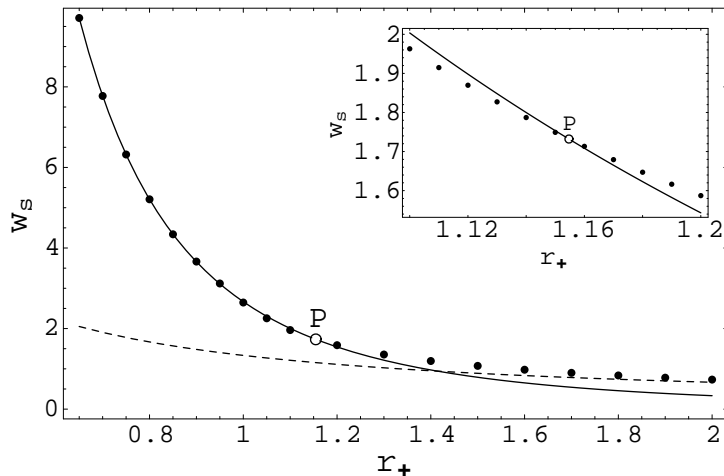


FIG. 2: The frequency  $\omega_s$  of the  $k = 2$  purely damped mode for intermediate and small black holes as a function of the horizon radius (the dots represent numerical results). The dashed line is  $\omega_s = 4/3r_+$ , and the solid line is the algebraically special frequency  $|\omega_a| = 8/3r_+^3$ . At point  $P = (2/\sqrt{3}, \sqrt{3})$ , the algebraically special frequency line crosses the purely damped QN frequency.

mode with  $k \geq \sqrt{3}r_+$ . A consequence of this for the numerical calculations is that, at  $r_+ = k/\sqrt{3}$ , our root-searching program based on the Horowitz-Hubeny method fails to find a pure imaginary QN frequency. The problem occurs when  $r_+$  approaches the point where the function  $\omega = i\omega_s(r_+)$  would intercept the algebraically special frequency  $\omega_a = ik^4/6r_+^3$ . This is indicated by the point P in Fig. 2, where we plot  $\omega_s$  as a function of  $r_+$  for  $k = 2$ . The numerical data show that  $\omega_s > |\omega_a|$  for all  $r_+ > k/\sqrt{3}$ , and  $\omega_s < |\omega_a|$  for all  $r_+ < k/\sqrt{3}$ .

| $n$ | Axial      |            | Polar      |            |
|-----|------------|------------|------------|------------|
|     | $\omega_r$ | $\omega_i$ | $\omega_r$ | $\omega_i$ |
| 1   | 184.948    | 266.384    | 184.963    | 266.351    |
| 2   | 316.130    | 491.641    | 316.159    | 491.583    |
| 3   | 446.438    | 716.753    | 446.482    | 716.671    |
| 4   | 576.528    | 941.807    | 576.586    | 941.700    |
| 5   | 706.536    | 1166.84    | 706.608    | 1166.71    |
| 20  | 2655.34    | 4541.91    | 2655.62    | 4541.40    |
| 40  | 5253.44    | 9041.92    | 5254.09    | 9041.02    |

TABLE V: QNMs corresponding to  $k = 2$  axial and polar perturbations of a large plane-symmetric AdS black hole, with  $r_+ = 100$ .

For small black holes, the purely damped frequency  $i\omega_s$  approaches the algebraically special frequency  $\omega_a$  from below. In fact, the difference between these frequencies is smaller than  $10^{-6}$  for  $r_+/k = 0.3$  and decreases as  $r_+/k \rightarrow 0$ . This conclusion has again its spherical counterpart, as it can be seen from the numerical results found in Ref. [31]. More details on the algebraically special frequency and on its non-QN character are given in Sec. VIII.

### C. Highly damped modes

For the moment, we present only the computed frequency values of the lowest QNMs. They are the most important modes for the AdS/CFT correspondence, since these give the thermalization time scale on the boundary field theory. However, as soon as one is interested in Hod's conjecture [51], which relates the classical QN frequencies with the quantum spectrum of black holes, the most relevant modes are the highly damped QNMs. Indeed, according to such a conjecture, the real part of the QN frequencies, in the limit of high overtones, gives information about the quantum of the black hole area. In the following, we present the QN frequency values for modes in the regime of high principal quantum numbers  $n$ . Since we can distinguish the purely damped modes as belonging to a special family, we simply label them with  $n = 0$ , and begin to label the fundamental ordinary modes with  $n = 1$ .



| $n$ | Axial      |            | Polar      |            |
|-----|------------|------------|------------|------------|
|     | $\omega_r$ | $\omega_i$ | $\omega_r$ | $\omega_i$ |
| 1   | 2.04735    | 2.21550    | 2.30526    | 1.55218    |
| 2   | 3.34678    | 4.74580    | 3.26137    | 3.72163    |
| 3   | 4.65907    | 7.05251    | 4.39306    | 5.96477    |
| 4   | 5.95653    | 9.32552    | 5.59513    | 8.21840    |
| 5   | 7.24999    | 11.5884    | 6.83055    | 10.4733    |
| 20  | 26.6726    | 45.3810    | 26.0793    | 44.2560    |
| 40  | 52.6238    | 90.3921    | 44.2193    | 75.7648    |

TABLE VI: QNMs corresponding to  $k = 2$  axial and polar perturbations of an intermediate size plane-symmetric AdS black hole, with  $r_+ = 1$ .

| $n$ | Axial      |            | Polar      |            |
|-----|------------|------------|------------|------------|
|     | $\omega_r$ | $\omega_i$ | $\omega_r$ | $\omega_i$ |
| 1   | 2.05667    | 0.214983   | 2.05678    | 0.214687   |
| 2   | 2.17823    | 0.576255   | 2.17845    | 0.575676   |
| 3   | 2.32373    | 0.974834   | 2.32406    | 0.974002   |
| 4   | 2.48740    | 1.39433    | 2.48783    | 1.39325    |
| 5   | 2.66559    | 1.82658    | 2.66613    | 1.82528    |
| 20  | 6.04295    | 8.60462    | 6.04536    | 8.60001    |
| 40  | 11.0316    | 17.6657    | 11.0366    | 17.6567    |

TABLE VII: QNMs corresponding to  $k = 2$  axial and polar perturbations of a small plane-symmetric AdS black hole, with  $r_+ = 0.2$ .

To study the QNMs asymptotic behavior, we computed the first 40 ordinary QN frequencies associated to  $k = 2$  axial and polar perturbations of plane-symmetric AdS black holes. A few representative results for some modes of large, intermediate, and small event horizons are displayed in Tables V, VI, and VII, respectively.

On the basis of this numerical data, we obtained linear fits by taking overtones from  $n = 21$  to  $n = 40$  and employing the discrete least squares approximation method. Together with the coefficients of the linear approximating functions, we calculated the error involved

| $r_+$ | Axial                  |                        | Polar                 |                        |
|-------|------------------------|------------------------|-----------------------|------------------------|
|       | $\alpha$               | $\beta$                | $\alpha$              | $\beta$                |
| 100   | $57.2447 + 41.9027i$   | $129.905 + 225.000i$   | $57.0927 + 41.7360i$  | $129.925 + 224.982i$   |
| 1     | $0.717273 + 0.371668i$ | $1.29763 + 2.25053i$   | $-7.58881 - 14.2636i$ | $1.29504 + 2.25074i$   |
| 0.2   | $1.02468 - 0.451644i$  | $0.249900 + 0.452989i$ | $1.02451 - 0.451813i$ | $0.250029 + 0.452767i$ |

TABLE VIII: Linear fits for the frequencies of high overtones of axial and polar perturbations for black holes with  $r_+ = 100$ ,  $r_+ = 1$ , and  $r_+ = 0.2$ .

in each fit process and established 1% as the upper bound error. This means that, in the regime of high overtones ( $n \rightarrow \infty$ ), the QN frequencies are evenly spaced with real and imaginary parts given approximately by linear functions as described below.

The linear fits depend upon the size of the horizon radius, and are given by functions of the form

$$\omega_n = \alpha + \beta n, \quad (24)$$

where the coefficients  $\alpha$  and  $\beta$  refer to both the real and the imaginary parts of the frequency, and are given in table VIII. Their dependence upon the black hole parameter  $r_+$  and on the wave number  $k$  is governed by Eq. (19).

As should be expected, the results found for large black holes reproduce those obtained in Ref. [31] for Schwarzschild-AdS black holes with a large event horizon. A special feature of the regime is that axial and polar perturbations have essentially the same QNM spectra, which appear in the first line of Table VIII. In the other regimes, however, the linear functions are very different from those of the spherical case.

The angular coefficients of the linear functions seem to present a kind of universal behavior. In fact, as seen from the  $\beta$  coefficients in Table VIII, the results for both of the perturbation types, and for each horizon radius, are very close to each other. The spacings between the frequencies per unit horizon radius of consecutive modes are essentially independent of the black hole size. This is seen more clearly in Table IX where the values of the ratio  $(\omega_{n+1} - \omega_n)/r_+$ , calculated for each regime, are shown. The data confirm that such a ratio, for the calculated wave number  $k = 2$ , is approximately constant. Additionally, using this result together with Eq. (23) it may be shown that, in the high overtones regime, the frequency per unit horizon radius spacing is not only independent of the black hole size and

|       | $(\omega_{n+1} - \omega_n)/r_+$ |                      |
|-------|---------------------------------|----------------------|
| $r_+$ | Axial                           | Polar                |
| 100   | $1.29905 + 2.25000i$            | $1.29925 + 2.24982i$ |
| 1     | $1.29763 + 2.25053i$            | $1.29504 + 2.25074i$ |
| 0.2   | $1.24950 + 2.26495i$            | $1.25015 + 2.26384i$ |

TABLE IX: The fractional spacing of frequencies among consecutive high overtones of axial and polar perturbations of black holes with  $r_+ = 100$ ,  $r_+ = 1$ , and  $r_+ = 0.2$ .

of the perturbation parity, but it is also independent of the wave-number value. The real parts for small black holes are about 4% lower than for intermediate and large black holes. We notice that this difference decreases as we search for overtones with principal quantum numbers much larger than  $n = 40$ , but we have not investigated this more precisely because the numerical calculations become very slow for overtones with  $n$  significantly larger than 40.

## VII. THE LARGE BLACK HOLE LIMIT OF THE PURELY DAMPED QNM

Although numerical procedures need to be used to compute the QN frequencies, it is possible to study analytically the special case of axial perturbations of very large black holes. Here we show in some detail the process of finding an asymptotic expression for the frequency of the purely damped modes. The analysis is performed in such a way that it holds for both the plane-symmetric and the Schwarzschild-AdS spacetimes.

Our starting point is the Horowitz-Hubeny approach described in Sec. V. There, the QN frequencies of axial perturbations are associated to solutions of the equation

$$\sum_{m=0}^{\infty} a_m(\omega) (-x_+)^m = 0. \quad (25)$$

Hence, we need to obtain an analytical expression for the sum of this series in order to find exact frequency values. Such a task is very difficult to be carried out for a general  $x_+$ , but it becomes feasible for the large black hole limit of purely damped modes.

The coefficients  $a_m(\omega)$  appearing in Eq. (25) are the Fröbenius coefficients of the power series solution to either Eq. (20) written for the axial functions, or the corresponding

equation in the Schwarzschild-AdS case (see Ref. [9]). They are given in terms of the frequency, and of the other physical parameters of the problem, by the following recurrence formulas:

$$a_1(-x_+)^1 = A_1 F_1 a_0(-x_+)^0, \quad (26)$$

$$a_m(-x_+)^m = \frac{F_m}{m} [A_m a_{m-1}(-x_+)^{m-1} - B_m a_{m-2}(-x_+)^{m-2}]. \quad (27)$$

The last equation is valid for all  $m \geq 2$  and we have shortened the equations by introducing the quantities

$$A_m = 3(m^2 - m - 1) + [q(q + \kappa) + (2m^2 - 2m - 3)\kappa] x_+^2, \quad (28)$$

$$B_m = (m^2 - 2m - 3) [1 + \kappa x_+^2], \quad (29)$$

$$F_m = [m(3 + \kappa x_+^2) + 2i\omega x_+]^{-1}, \quad (30)$$

where  $q = k, l$  and  $\kappa = 0, 1$  depending on whether it is considered a plane or spherical hole, respectively, and now the foregoing expressions hold for any  $m \geq 1$ .

In the large black hole regime, the wave number (or the angular momentum) of the perturbation is negligible and the frequency scales as  $\omega \sim 1/x_+$ . In terms of the variable  $x_+$ , it implies that  $\omega$  has a first order pole at  $x_+ = 0$ . Therefore,  $\omega(x_+)$  has a Laurent series about  $x_+ = 0$ , which is valid over the range  $0 < x_+ < R$ , for some  $R$  [50]. Such an expansion can be conveniently written as  $-2ix_+\omega = \sum_{m=0}^{\infty} b_m x_+^m$ , where  $b_m$  are constants to be determined. However, not all of the elements  $b_m$  are independent, since part of them can be eliminated on the basis of the parity property of the function  $\omega(x_+)$ . Independently of what results from the sum on the left-hand side of Eq. (25), the form of the quantities  $A_m$ ,  $B_m$ , and  $F_m$  ensures that the product  $x_+\omega$  is a function of  $x_+^2$ . This means that  $\omega$  changes its sign under the transformation  $x_+ \rightarrow -x_+$ , being an odd function of  $x_+$ . Accordingly, the series representing  $x_+\omega$  should be an even function of  $x_+$ , which means that only the even powers of  $x_+$  should survive, and then one should have  $b_{2n+1} = 0$  for all  $n \geq 0$ . This result allows us to write

$$-2ix_+\omega = \sum_{m=0}^{\infty} c_m z^m, \quad (31)$$

where  $z = x_+^2$  and  $c_m$  are constants to be determined.

The series representation of  $2ix_+\omega$  opens the possibility of Taylor expanding the terms  $a_m(-x_+)^m$  about  $z = 0$ . Before doing this, we notice that the value of  $a_0$  is arbitrary, since

all the terms in the series of Eq. (25) are proportional to this element and the full sum is equal to zero. For simplicity, we choose here  $a_0 = 1$ . Then we substitute Eq. (31) into Eq. (30) and expand  $F_m$  (which depends on  $x_+$  and also on  $\omega$ ) about  $z = 0$ . When this expansion is substituted back into Eqs. (26) and (27), we obtain a set of Taylor series for the elements  $a_m(-x_+)^m$  (one of such series for each  $m$ ), which may be represented by

$$a_m(-x_+)^m = \sum_{j=0}^{\infty} \eta_m^j z^j,$$

where the elements  $\eta_m^j$  are functions of  $q, \kappa, c_0, c_1, \dots, c_j$ . Substituting the previous expansions into Eq. (25) and collecting terms of the same power in  $z$ , we find

$$[1 + \eta_1^0(c_0) + \eta_2^0(c_0) + \dots] + [\eta_1^1(c_0, c_1) + \eta_2^1(c_0, c_1) + \dots] z + \dots = 0. \quad (32)$$

Yet the left-hand side of Eq. (32) is a power series in the variable  $z$ . It implies that, in order for the equation being satisfied, all bracketed terms should vanish. Therefore, the zeroth order coefficient provides an equation for  $c_0$ , the first order coefficient, together with the earlier calculated value of  $c_0$ , provides an equation for  $c_1$ , and so on. Here we begin with the computations that lead to  $c_0$ . The first two relevant terms for this task are  $\eta_1^0 = -3/(3 - c_0)$  and  $\eta_2^0 = -3c_0/[2(3 - c_0)(6 - c_0)]$ . Moreover, it can be seen from Eq. (29) that  $B_3$  is identically zero, and as a consequence the term  $a_3(-x_+)^3$  differs from  $a_2(-x_+)^2$  only by a multiplicative factor. This implies, in particular, that the element  $\eta_3^0$  is related to  $\eta_2^0$  by  $\eta_3^0 = 5/(9 - c_0)\eta_2^0$ . Such a relation, together with the formulas (26) and (27), implies that all the subsequent elements are also proportional to  $\eta_2^0$ . More specifically, the  $m$ th coefficient (for  $m \geq 2$ ) can be written as  $\eta_m^0 = \gamma_m(c_0)\eta_2^0$ , where  $\gamma_m(c_0)$  is given by the recurrence formula

$$\gamma_m(c_0) = \frac{1}{m(3m - c_0)} [3(m^2 - m - 1)\gamma_{m-1}(c_0) - (m^2 - 2m - 3)\gamma_{m-2}(c_0)],$$

with  $\gamma_2(c_0) = 1$  and  $\gamma_3(c_0) = 5/9$ .

Taking into account the last results, the  $z$ -independent term of Eq. (32) gives rise to the following equation for  $c_0$ :

$$c_0 \left[ \frac{1}{(3 - c_0)} + \frac{3}{2(3 - c_0)(6 - c_0)} \sum_{m=2}^{\infty} \gamma_m(c_0) \right] = 0. \quad (33)$$

Clearly the above equation has the special solution  $c_0 = 0$ , in addition to the roots that arise as zeros of the square-bracketed term. The existence of this special solution explains

why the purely damped modes do not scale with the horizon size, as it happens to ordinary modes in the large black hole limit. In fact, the numerical computations show that purely damped modes are the only QNMs which in first approximation are not proportional to  $r_+$ . This fact suggests they should be associated to the root  $c_0 = 0$ , and then it follows from Eq. (31) that for large horizon radii the corresponding frequencies go as  $1/r_+$ . On the other hand, the numerical results also indicate that the ordinary axial QNMs are proportional to  $r_+$  (in first approximation). From this one concludes that the remaining roots that are obtained from the zeros of the term among brackets in Eq. (33) correspond to the asymptotic values of the function  $2ix_+ \omega$  for these ordinary QNMs.

It is seen from the above analysis that, in order to calculate the leading term of the large horizon limit for the purely damped mode frequency, we must take  $c_0 = 0$  and calculate the next parameter  $c_1$ . In such a case, the coefficients  $\eta_1^1$  and  $\eta_2^1$  reduce to  $\eta_1^1 = [q(q + \kappa) - 2\kappa - c_1]/3$  and  $\eta_2^1 = -c_1/12$ , while the other elements  $\eta_m^1$  (for  $m \geq 3$ ) assume the form  $\eta_m^1 = \gamma_m(0)\eta_2^1$ . Substituting these results into the first order coefficient of (32) we obtain an equation that can be solved for  $c_1$ , yielding

$$c_1 = \frac{4[q(q + \kappa) - 2\kappa]}{(4 + \gamma)},$$

where we have defined

$$\gamma = \sum_{m=0}^{\infty} \gamma_m(0). \quad (34)$$

The problem now is summing the series that leads to  $\gamma$ . Fortunately, we succeeded in summing up this series (see Appendix B) and the exact result is  $\gamma = 2$ . With this, the coefficient  $c_1$  becomes

$$c_1 = \frac{2}{3}(q - q_-)(q - q_+),$$

where  $q_-$  and  $q_+$  are given by

$$q_{\pm} = \frac{-\kappa \pm \sqrt{\kappa^2 + 8\kappa}}{2}. \quad (35)$$

Once we have obtained an expression for  $c_1$ , the asymptotic formula of the pure imaginary QN frequency follows directly from Eq. (31). In fact, considering a plane-symmetric AdS black hole, for which  $q = k$  and  $\kappa = 0$ , we have  $q_- = q_+ = 0$ , and the interesting result follows:

$$\omega = i \frac{k^2}{3r_+}.$$

Alternatively, for a Schwarzschild-AdS black hole one has  $q = l$  and  $\kappa = 1$ , which implies in  $q_- = 1$  and  $q_+ = -2$ , leading to

$$\omega = i \frac{(l-1)(l+2)}{3r_+}.$$

Both of the last two formulas for the purely damped frequencies are exact results at the asymptotic limit of large black holes, in perfect agreement with the approximate fits found through the numerical calculations.

### VIII. ALGEBRAICALLY SPECIAL MODES

The numerical results of the QN frequencies revealed a close relation between the algebraically special modes and the purely damped QNMs. For a fixed wave number, the imaginary frequency  $\omega = i\omega_s$  approaches the values of the special frequency  $\omega_a$  as the horizon radius goes to zero (see the comments at the end of section III). There also seems to exist a meeting point P between the two frequencies for a special combination of parameters such that  $V^{(-)}(r_+)/f(r_+) = 0$ , as it can be seen from the numerical results shown in Fig. 2. Furthermore, the relation between the purely damped modes and the algebraically special frequency in the small horizon limit is not restricted to the plane-symmetric black hole case, but it also appears in axial perturbations in the Schwarzschild-AdS spacetime. All these facts render it convenient to analyze here the QN character of the algebraically special perturbation modes. The frequency function of these modes for the plane-symmetric black hole is given by Eq. (14), while the corresponding expression in the spherical case is found in Ref. [12]. In a general form, the frequency  $\omega_a$  can be written as

$$\omega_a = i \frac{q(q+\kappa)[q(q+\kappa) - 2\kappa]}{6(1 + \kappa x_+^2)} x_+^3,$$

where again  $q = k, l$  and  $\kappa = 0, 1$ , as it is considered a plane or spherical black hole, respectively.

To verify if the algebraically special modes satisfy the QNM boundary conditions we need to obtain the solution  $\phi_a^{(-)}(x)$  associated with the algebraically special frequency  $\omega_a$ . Since this function is a particular case of the general power series solution (21), we may use Eqs. (26) and (27) to determine the coefficients  $a_m$  for  $\omega = \omega_a$ . Once again we may take  $a_0 = 1$ ,

so that the coefficients  $a_1$  and  $a_2$  are given, respectively, by

$$a_1 = \frac{3(1 + \kappa x_+^2) - q(q + \kappa)x_+^2}{x_+(3 + \kappa x_+^2 + 2i\omega x_+)},$$

$$a_2 = \frac{x_+^3 q(q + \kappa)[q(q + \kappa) - 2\kappa] + 6i\omega(1 + \kappa x_+^2)}{4x_+(3 + \kappa x_+^2 + i\omega x_+)(3 + \kappa x_+^2 + 2i\omega x_+)}.$$

It is seen from the last equation that  $a_2$  vanishes for the frequency  $\omega = \omega_a$ . Moreover, since all the other elements  $a_m$  (for  $m \geq 3$ ) differ from  $a_2$  only by a multiplicative factor, we have  $a_3 = a_4 = \dots = 0$ . The solution for  $\phi_a^{(-)}(x)$  then reduces to

$$\phi_a^{(-)}(x) = 1 - \frac{3(1 + \kappa x_+^2)}{3 + [q(q + \kappa) + \kappa]x_+^2} \left(1 - \frac{x}{x_+}\right). \quad (36)$$

We know from the Horowitz-Hubeny method that the function (36) represents an ingoing wave at the event horizon. Here the problem is verifying if  $\phi_a^{(-)}(x)$  satisfies the Dirichlet boundary condition at the spatial infinity. Imposing the condition  $\phi_a^{(-)}(0) = 0$ , we find an equation that is satisfied only if  $q = q_+$  or  $q = q_-$ , where  $q_+$  and  $q_-$  are given by Eq. (35). For a plane-symmetric AdS black hole, this means we need a vanishing wave number in order to have a QN frequency equal to  $\omega_a$ . In this case, however, the resulting perturbation functions would be independent of time, which could not represent gravitational waves. Similarly, for a Schwarzschild-AdS spacetime we need to have  $l = -2$  or  $l = 1$ . The first root is a physically forbidden value, while the second one leads to a static perturbation, which only adds a small rotation to the black hole [52]. On the basis of these results, we conclude that  $\omega_a$  cannot be a QN frequency, because the associated wave function  $\phi_a^{(-)}(x)$  does not satisfy the Dirichlet boundary condition at infinity.

Although the numerical calculations show that in the small horizon limit  $\omega = i\omega_s$  is very close to  $\omega_a$ , the above result proves that the frequency function associated with purely damped modes is not exactly equal to the algebraically special frequency. The solid line in Fig. 2 does not coincide with the dots, which represent QNMs, not even in the small black hole regime. There is, however, a special point P where  $\omega_a$  seems to coincide with  $i\omega_s$ . The answer to the question whether  $\omega_a$  corresponds to a QN frequency at that point or not is given in the following.

In spite of the generality of the analysis performed above, it fails to test the QN character of  $\omega_a$  in the case where  $V^{(-)}(r_+)/f(r_+) = 0$ . This situation happens for a special family of parameters satisfying the condition

$$q(q + \kappa) = \frac{3(1 + \kappa x_+^2)}{x_+^2}. \quad (37)$$



In this case the roots of the Fröbenius index equation, which are  $\alpha = 0$  and  $\alpha = 2i\omega/f'(r_+) = 1$  ( $f' \equiv df/dr$ ), differ by an integer number and the Horowitz-Hubeny method is not valid. We can circumvent this problem by writing explicitly the axial version of Eq. (20) for  $\omega = \omega_a$  and parameters satisfying Eq. (37). By doing this in such a way that the analysis holds for both the plane and the spherical AdS black holes, it is found that

$$\left[ (1 + \kappa x_+^2)x^2 + x_+x + x_+^2 \right] \frac{d^2\phi_a^{(-)}}{dx^2} + \left[ 3(1 + \kappa x_+^2)x + (3 + \kappa x_+^2)x_+ \right] \frac{d\phi_a^{(-)}}{dx} - 3(1 + \kappa x_+^2)\phi_a^{(-)} = 0. \quad (38)$$

Here  $x = x_+$  is a regular point of the above differential equation, and the solution for  $\phi_a^{(-)}$  can be expressed as a Taylor series,

$$\phi_a^{(-)}(x) = \sum_{m=0}^{\infty} d_m (x - x_+)^m.$$

Substituting this expression into Eq. (38), we find as usual that all coefficients  $d_m$  (for  $m \geq 2$ ) can be expressed in terms of the first two,  $d_0$  and  $d_1$ . The general solution of Eq. (38) then assumes the form

$$\begin{aligned} \phi_a^{(-)}(x) = & d_0 \left[ 1 + \frac{3(1 + \kappa x_+^2)}{2(3 + \kappa x_+^2)} \sum_{m=2}^{\infty} \frac{\beta_m}{(-x_+)^m} (x - x_+)^m \right] \\ & + d_1 \left[ (x - x_+) + \frac{(3 + 2\kappa x_+^2)}{(3 + \kappa x_+^2)} \sum_{m=2}^{\infty} \frac{\beta_m}{(-x_+)^{m-1}} (x - x_+)^m \right], \end{aligned} \quad (39)$$

where the parameters  $\beta_m$  (for all  $m \geq 4$ ) are given by the recurrence formula

$$\beta_m = \frac{(3 + 2\kappa x_+^2)}{(3 + \kappa x_+^2)} \beta_{m-1} - \frac{(m-3)(m+1)(1 + \kappa x_+^2)}{m(m-1)(3 + \kappa x_+^2)} \beta_{m-2},$$

with  $\beta_2 = 1$  and  $\beta_3 = (3 + 2\kappa x_+^2)/(3 + \kappa x_+^2)$ .

The first term among brackets in Eq. (39) represents a perturbation function which is constant at the event horizon and corresponds to an ingoing wave, while the second term represents an outgoing wave, since it goes as  $(x - x_+)$  in the limit  $x \rightarrow x_+$ . To satisfy the QNM boundary condition at the horizon, we must take  $d_1 = 0$  and keep only the first term of the general solution (39). In addition, without loss of generality we may choose  $d_0 = 1$ . Finally, we must verify if the function  $\phi_a^{(-)}(x)$  satisfies the Dirichlet boundary condition at the spatial infinity  $x = 0$ . By substituting  $d_0 = 1$ ,  $d_1 = 0$ , and  $x = 0$  into Eq. (39) it follows that

$$\phi_a^{(-)}(0) = 1 + \frac{3(1 + \kappa x_+^2)}{2(3 + \kappa x_+^2)} \sum_{m=2}^{\infty} \beta_m \equiv \phi_{\infty}(\kappa, x_+).$$

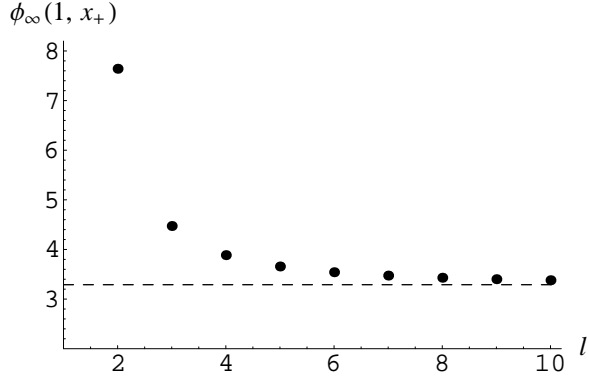


FIG. 3: The values of  $\phi_\infty(1, x_+)$  as a function of the angular momentum  $l$ . The dots are numerical results, while the dashed line is  $\phi_\infty(0, x_+) \simeq 3.29$ .

For plane-symmetric AdS black holes, our numerical calculations show that  $\phi_\infty(0, x_+) \simeq 3.29$ , independently of the horizon radius. On the other hand, we obtain different values for  $\phi_\infty(1, x_+)$  as we change the Schwarzschild black hole size. Another way to see this variation is in terms of the angular momentum, since  $x_+$  and  $l$  are coupled through Eq. (37). In Fig. 3, we plot the numerical values of  $\phi_\infty(0, x_+)$  (dashed line) and of  $\phi_\infty(1, x_+)$  for  $l \geq 2$  (dots). As the angular momentum goes to infinity, which means  $x_+ \rightarrow 0$ , the results found for the spherical case tend to the value of the plane black hole. Since  $\phi_\infty(\kappa, x_+)$  is always different from zero, we conclude that the algebraically special modes are not QNMs, not even for the special parameters that lead to  $V^{(-)}(r_+)/f(r_+) = 0$ . For the plane-symmetric black hole and for  $k = 2$ , this corresponds to the point P in Fig. 2, where the lines representing the purely damped QN and the algebraically special frequencies tend to intercept each other. Among other things, this result implies that the QNM spectrum of some black holes does not present a particular pure imaginary frequency, for those specific modes whose wave numbers (or angular momentum) satisfy Eq. (37). For instance, an axial quadrupole ( $l = 2$ ) perturbation is not able to excite a purely damped QNM in a Schwarzschild-AdS black hole with  $r_+ = 1$ . Whether this conclusion has some physical implication to the AdS/CFT conjecture or not is still an open question.

## IX. FINAL COMMENTS AND CONCLUSION

We have studied the gravitational quasinormal modes of plane-symmetric anti-de Sitter black holes. These modes are responsible for the late time behavior of small gravitational disturbances. The wave equations governing the axial and polar perturbations were derived by a procedure based on the Newman-Penrose formalism and on the Chandrasekhar transformation theory. This approach allowed us to treat equally the two spacelike coordinates  $\varphi$  and  $z$ , as well as provided the algebraically special frequencies associated to the gravitational waves radiated by the black hole.

Using the Horowitz-Hubeny method, we have computed the quasinormal frequencies for  $k = 2$  and several values of  $r_+$  in the large, intermediate, and small black hole regimes. The wave-number dependence of the modes was obtained on the basis of the homogeneity property of the function  $\omega(r_+, k)$ . For large black holes, the ordinary frequencies scale linearly with  $r_+$ , and the pure imaginary frequency goes as  $1/r_+$ . For small black holes, the fundamental modes present  $\omega_r \rightarrow k$  and  $\omega_i \rightarrow 0$ , while  $\omega = i\omega_s$  approaches the algebraically special frequency  $\omega_a = ik^4/6r_+^3$ . In the limit of highly damped overtones, we found the QN frequencies are evenly spaced, with the spacing per unit of horizon radius being a constant which is independent of the wave-number value, perturbation parity, and black hole size.

In relation to stability, we have shown analytically that for a non-negative potential the imaginary part of the frequency is positive definite for every mode. From the numerical results it also follows that all QN frequencies have a positive imaginary part, including the cases where the potential takes negative values. These results conjointly imply that plane-symmetric AdS black holes are stable against gravitational perturbations.

To study the large black hole limit we have developed an analytical method based on the expansion of the frequency in powers of  $1/r_+$ . Application of this method to axial perturbations showed that there is a special frequency for which the ratio  $\omega/r_+$  goes to zero as  $r_+ \rightarrow \infty$ . The first nonvanishing term is  $\omega_s = ik^2/3r_+$  for the plane hole and  $\omega_s = i(l-1)(l+2)/3r_+$  for the Schwarzschild hole. It is important to observe that these purely damped modes are particularly long living for large black holes, which is exactly the relevant regime for the AdS/CFT correspondence. If the above asymptotic formulas could be derived on the CFT side, it could provide an important quantitative test to the Maldacena's conjecture.

As a last remark, it should be noted that the discussion of the physical interpretation of the modes with different wave-number values remains. Preliminary results show that the zero wave-number axial perturbations yield only small rotations on the system, while the polar ones lead to an increase in the mass and the production of gravitational waves [53]. This issue, however, must be investigated in more detail and shall be considered in our future work.

### Acknowledgments

We are indebted to V. Cardoso for suggestions and for a critical reading of the manuscript. We also thank J. P. S. Lemos for stimulating conversations. One of us (A. S. M.) thanks the Conselho Nacional de Desenvolvimento Científico e Tecnológico - CNPq, Brazil, for a grant.

## APPENDIX A: THE PURE AdS PLANE-SYMMETRIC GRAVITATIONAL MODES

In this appendix we discuss briefly how to find the modes of gravitational perturbations in pure plane-symmetric AdS spacetimes. This is to be compared to the small black hole limit QNMs, as calculated numerically in Sec. VI.

The relevant wave equations for axial and polar perturbations may be obtained from Eq. (10) by assuming  $M = 0$  wherever it appears. For instance, the potentials  $V^{(\pm)}$  reduce to the same constant value

$$V^{(\pm)} = k^2. \quad (\text{A1})$$

The resulting equations are then

$$\left( \frac{d^2}{dr_*^2} + \omega^2 - k^2 \right) Z^{(\pm)} = 0, \quad (\text{A2})$$

whose solutions in terms of the coordinate  $r = 1/r_*$  are of the form

$$Z^{(\pm)} = \begin{cases} a^{(\pm)} e^{i\sqrt{\omega^2 - k^2}/r} + b^{(\pm)} e^{-i\sqrt{\omega^2 - k^2}/r}, & \omega^2 \neq k^2, \\ \frac{c^{(\pm)}}{r} + d^{(\pm)}, & \omega^2 = k^2, \end{cases} \quad (\text{A3})$$

where  $a^{(\pm)}$ ,  $b^{(\pm)}$ ,  $c^{(\pm)}$ , and  $d^{(\pm)}$  are integration constants.

The solution functions for  $\omega^2 \neq k^2$  are analytic in the whole range of the radial coordinate which is of interest for comparison to the small black hole QNMs,  $0 < r < \infty$ . Hence, the only condition  $\omega$  must satisfy is

$$\omega^2 > k^2 \tag{A4}$$

in order to avoid the wave growing exponentially in the limit  $r \rightarrow 0$ .

However, additional restrictions to these modes arise by imposing the usual boundary conditions for QNMs in AdS spacetimes: no wave can come out from the black hole horizon, which is located at  $r = r_+ \rightarrow 0$ ; and no wave can propagate to spatial infinity,  $r \rightarrow \infty$ . By substituting these conditions into Eqs. (A3) it follows that  $a^{(\pm)} = 0$  and  $b^{(\pm)} = 0$ , which means waves whose frequencies satisfy the relation  $\omega^2 \neq k^2$  do vanish everywhere.

We are then left with the solutions for which  $\omega^2 = k^2$  only. In this case there is in fact no wave in the radial direction, so that the solutions  $Z^\pm = c^{(\pm)}/r + d^{(\pm)}$ , for  $r > 0$ , represent waves traveling along the spatial directions orthogonal to the  $r$  direction. In other words, there are no waves coming out from the horizon nor propagating to spacelike infinity. Considering these as the plane-symmetric pure AdS modes, their frequencies, given by

$$\omega = k,$$

agree with the result found numerically for small black holes.

## APPENDIX B: SUMMATION OF THE SERIES FOR MODES OF LARGE BLACK HOLES

Here we show how the series presented in Eq. (34) can be summed up exactly. Since it is an alternating series, it is important not only to prove its convergence, but also to test it for absolute convergence. By mathematical induction, we find that the series (34) can be written as a combination of seven terms

$$\gamma = 2 + \sum_{m=1}^{\infty} \alpha_m^1 + \sum_{m=1}^{\infty} \alpha_m^2 + \sum_{m=1}^{\infty} \alpha_m^3 + \sum_{m=1}^{\infty} \alpha_m^4 + \sum_{m=1}^{\infty} \alpha_m^5 + \sum_{m=1}^{\infty} \alpha_m^6, \tag{B1}$$

where the elements  $\alpha_m^i$  ( $i = 1, 2, \dots, 6$ ) are given by

$$\begin{aligned}\alpha_m^1 &= (-1)^m \frac{2}{3^{3m+2}(6m+5)}, & \alpha_m^2 &= (-1)^{m+1} \frac{2}{3^{3m}(6m+1)}, \\ \alpha_m^3 &= (-1)^m \frac{1}{3^{3m}(6m+1)(3m+1)}, & \alpha_m^4 &= (-1)^m \frac{6m+5}{3^{3m+2}(3m+1)(2m+1)}, \\ \alpha_m^5 &= (-1)^m \frac{6m+5}{3^{3m+2}(3m+2)(2m+1)}, & \alpha_m^6 &= (-1)^m \frac{12m+11}{3^{3m+2}(3m+2)(6m+5)}.\end{aligned}$$

Then we are left with a sum of six series, and by proving the absolute convergence of each one of them, the absolute convergence of the whole series  $\sum_m \gamma_m(0)$  is also proved. In order to do that, we calculate the limit

$$\lim_{m \rightarrow \infty} \frac{|\alpha_{m+1}^i|}{|\alpha_m^i|} = \frac{1}{3^3}$$

and verify that it is smaller than unity for any  $i$ , and then by applying the D'Alembert ratio test we conclude that every individual series is absolutely convergent. This result implies that the final sum for  $\gamma$  is independent of the element ordering in the alternating series. In particular, we can add the terms  $\alpha_m^i$  over all  $i$ , for  $i = 1, 2, \dots, 6$ , before performing the sum over  $m$ . By doing that, we find the simple result  $\sum_i \alpha_m^i = 0$  for any value of  $m$ , and hence the sum over  $m$  gives zero. Therefore, the sum of the series (B1) is  $\gamma = 2$ .

- 
- [1] R.F. Stark and T. Piran, Phys. Rev. Lett. **55**, 891 (1985).
  - [2] P. Anninos, D. Hobill, E. Seidel, L. Smarr, and W.-M. Suen, Phys. Rev. Lett. **71**, 2851 (1993).
  - [3] K.D. Kokkotas and B.G. Schmidt, Living Rev. Relativity **2**, 2 (1999), <http://livingreviews.org/Articles/Volume2/1999-2kokkotas/>.
  - [4] G.T. Horowitz and V.E. Hubeny, Phys. Rev. D **62**, 024027 (2000).
  - [5] J.M. Maldacena, Adv. Theor. Math. Phys. **2**, 231 (1998).
  - [6] O. Aharony, S.S. Gubser, J.M. Maldacena, H. Ooguri, and Y. Oz, Phys. Rep. **323**, 183 (2000).
  - [7] J.S.F. Chan and R.B. Mann, Phys. Rev. D **55**, 7546 (1997).
  - [8] J.S.F. Chan and R.B. Mann, Phys. Rev. D **59**, 064025 (1999).
  - [9] V. Cardoso and J.P.S. Lemos, Phys. Rev. D **64**, 084017 (2001).
  - [10] T.R. Govindarajan and V. Suneeta, Classical Quantum Gravity **18**, 265 (2001).
  - [11] R.A. Konoplya, Phys. Rev. D **66**, 044009 (2002).
  - [12] I.G. Moss and J.P. Norman, Classical Quantum Gravity **19**, 2323 (2002).

- [13] S. Musiri and G. Siopsis, Phys. Lett. B **563**, 102 (2003).
- [14] M. Giammatteo and J. Jing, Phys. Rev. D **71**, 024007 (2005).
- [15] J.-L. Jing, gr-qc/0502010.
- [16] B. Wang, C.-Y. Lin and E. Abdalla, Phys. Lett. B **481**, 79 (2000).
- [17] R.A. Konoplya, Phys. Rev. D **66**, 084007 (2002).
- [18] E. Berti and K.D. Kokkotas, Phys. Rev. D **67**, 064020 (2003).
- [19] R.A. Konoplya, Phys. Rev. D **68**, 124017 (2003).
- [20] J.-L. Jing and Q.-Y. Pan, Phys. Rev. D **71**, 124011 (2005).
- [21] V. Cardoso, O.J.C. Dias, J.P.S. Lemos, and S. Yoshida, Phys. Rev. D **70**, 044039 (2004).
- [22] V. Cardoso and O.J.C. Dias, Phys. Rev. D **70**, 084011 (2004).
- [23] M. Giammatteo and I.G. Moss, Classical Quantum Gravity **22**, 1803 (2005).
- [24] M. Bañados, C. Teitelboim, and J. Zanelli, Phys. Rev. Lett. **69**, 1849 (1992).
- [25] V. Cardoso and J.P.S. Lemos, Phys. Rev. D **63**, 124015 (2001).
- [26] D. Birmingham, I. Sachs, and S.N. Solodukhin, Phys. Rev. Lett. **88**, 151301 (2002).
- [27] B. Wang, C. Molina, and E. Abdalla, Phys. Rev. D **63**, 084001 (2001).
- [28] J.-M. Zhu, B. Wang, and E. Abdalla, Phys. Rev. D **63**, 124004 (2001).
- [29] B. Wang, E. Abdalla, and R.B. Mann, Phys. Rev. D **65**, 084006 (2002).
- [30] B. Wang, C.-Y. Lin, and C. Molina, Phys. Rev. D **70**, 064025 (2004).
- [31] V. Cardoso, R.A. Konoplya, and J.P.S. Lemos, Phys. Rev. D **68**, 044024 (2003).
- [32] S. Musiri and G. Siopsis, Phys. Lett. B **576**, 309 (2003).
- [33] G. Siopsis, Phys. Lett. B **590**, 105 (2004).
- [34] V. Cardoso, J. Natário, and R. Schiappa, J. Math. Phys. (N.Y.) **45**, 4698 (2004).
- [35] J. Natário and R. Schiappa, hep-th/0411267.
- [36] M.R. Setare, Classical Quantum Gravity **21**, 1453 (2004).
- [37] V. Cardoso and J.P.S. Lemos, Classical Quantum Gravity **18**, 5257 (2001).
- [38] E.T. Newman and R. Penrose, J. Math. Phys. (N.Y.) **3**, 566 (1962).
- [39] S. Chandrasekhar, *The Mathematical Theory of Black Holes* (Oxford University Press, New York, 1983).
- [40] D. Kramer, H. Stephani, E. Herlt, and M. MacCallum, *Exact Solutions of Einstein's Field Equations* (Cambridge University Press, Cambridge, England, 1980).
- [41] C.-G. Huang and C.-B. Liang, Phys. Lett. A **201**, 27 (1995).

- [42] J.P.S. Lemos, Phys. Lett. B **353**, 46 (1995).
- [43] J.P.S. Lemos and V.T. Zanchin, Phys. Rev. D **54** 3840 (1996).
- [44] R.-G. Cai and Y.-Z. Zhang, Phys. Rev. D **54**, 4891 (1996).
- [45] W. Kinnersley, J. Math. Phys. (N.Y.) **10**, 1195 (1969).
- [46] S.A. Teukolsky, Astrophys. J. **185**, 635 (1973).
- [47] A.A. Starobinsky, Zh. Eksp. Teor. Fiz. **64**, 48 (1973)[Sov. Phys. JETP **37**, 28 (1974)].
- [48] S. Chandrasekhar, Proc. R. Soc. A **392**, 1 (1984).
- [49] S.J. Avis, C.J. Isham, and D. Storey, Phys. Rev. D **18**, 3565 (1978).
- [50] E. Butkov, *Mathematical Physics* (Addison-Wesley, Reading, MA, 1968).
- [51] S. Hod, Phys. Rev. Lett. **81**, 4293 (1998).
- [52] F.J. Zerilli, Phys. Rev. D **2**, 2141 (1970).
- [53] A.S. Miranda and V.T. Zanchin, “Gravitational Perturbations and Quasinormal Modes of Black Holes with Non-spherical Topology,” Int. J. Mod. Phys. D (to be published).